GEOPHYSICAL RESEARCH LETTERS, VOL. 28, NO. 10, PAGES 1957-1960, MAY 15, 2001

The loss of NO_2, HNO_3, NO_3/N_2O_5, and $HO_2/HOONO_2$ on soot aerosol: A chamber and modeling study

H. Saathoff, K.-H. Naumann, N. Riemer, S. Kamm, O. Möhler, U. Schurath, H. Vogel and B. Vogel

Institut für Meteorologie und Klimaforschung, Forschungszentrum Karlsruhe, POB 3640, D-76021 Karlsruhe, Germany

Abstract. The heterogeneous loss of NO_2, HNO_3, NO_3 / N_2O_5, and HO_2 / HO_2NO_2 on soot aerosol was investigated in a large aerosol chamber for interaction times of up to several days. By fitting a detailed model to the measured time profiles of the trace gas concentrations in the presence / absence of soot aerosol, the following reaction probabilities have been deduced at 294 K and <10 ppm H_2O (in parentheses: at 50% r.h.): $\gamma(NO_2) \leq 4\times10^{-8}$; $\gamma(HNO_3 \rightarrow NO_2) \leq 3\times10^{-7}$; $\gamma(NO_3) \leq 3\times10^{-4}$ ($\leq 10^{-3}$); $\gamma(N_2O_5$, hydrolysis) = $(4\pm2)\times10^{-5}$ ($(2\pm1)\times10^{-4}$); $\gamma(N_2O_5$, reduction) = $(4\pm2)\times10^{-6}$; $\gamma(HO_2) \leq 10^{-2}$; $\gamma(HO_2NO_2) \leq 10^{-5}$. These results were adopted in a series of box model calculations for four-day summer smog episodes, probing a wide range of NO emission rates. The 2nd day ozone maxima were reduced up to 10 % in the presence of 20 $\mu g\ m^{-3}$ soot aerosol, mainly due to the heterogeneous loss of HO_2.

Introduction

Soot particles are formed by incomplete combustion of carbonaceous fuels. Diesel engines are the main anthropogenic source, which contributes up to 10 $\mu g\ m^{-3}$ soot to the aerosol load in polluted urban areas (Israel et al., 1996). Concentrations of several 100 $ng\ m^{-3}$ have been reported for continental background air (Pakkanen et al., 2000). In northern hemispheric flight corridors soot particle number densities in the order of $10^5\ m^{-3}$ have been detected (Petzold et al., 1999).

In addition to their toxic properties, soot particles are of environmental concern because of their impact on climate (Jacobson, 2000; Hansen et al., 2000). Since the fractal structure of soot particles offers a large specific surface area for heterogeneous reactions with trace gases, attempts have been made in recent years to quantify their impact on the chemistry of the atmosphere (Jacob, 2000). Several laboratories have reported reaction probabilities γ for a number of atmospheric trace gases (e.g. Stephens et al., 1986; Brouwer et al., 1986; Fendel et al., 1995; Kalberer et al., 1996; Rogaski et al., 1997) which imply that soot aerosol may cause significant direct ozone loss (Bekki, 1997, Strawa et al., 1999) and affect the NO_x / NO_y ratio by reducing HNO_3 and NO_2 (Hauglustaine et al., 1996; Lary et al., 1997; Aumont et al., 1999). However, these model predictions are based on constant reaction probabilities, while soot particles may become considerably less reactive on atmospheric time scales due to surface ageing (Kamm et al., 1999; Disselkamp et al., 2000a,b; Kirchner et al., 2000). Furthermore, it has been shown (Underwood et al., 2000) that certain laboratory techniques tend to overpredict low reaction probabilities on aerosol particles by orders of magnitude.

Paper number 2000GL012619.
0094-8276/01/2000GL012619$05.00

Experimental and Modeling

We have investigated the interactions of airborne soot particles with a number of trace gases using the large evacuable aerosol chamber AIDA which provides excellent control of temperature, pressure, and humidity (Kamm et al., 1999). The large volume of 84 m^3 allows experiments to be carried out under close to atmospheric conditions on time scales of several days, approaching typical residence times of atmospheric aerosols.

The standard procedure to determine reactive losses of a trace gas on soot aerosol was as follows: First the temporal evolution of the trace gas was measured in particle-free air to determine wall losses. Then the experiment was repeated in the presence of soot aerosol. Finally possible changes of wall conditions were examined by repeating the first experiment in the absence of soot aerosol. Wall losses were minimized by preconditioning the chamber with 100 ppm ozone and N_2O_5/HNO_3. They changed negligibly between experiments in most cases. Before each experiment the chamber was evacuated to 0.02 hPa, flushed twice with 10 hPa synthetic air, and filled with synthetic air to ambient pressure. Then ca. 200 $\mu g\ m^{-3}$ soot aerosol was added from a graphite spark generator (GfG 1000, Palas). In the next step a trace gas was added. A fan was used for rapid mixing.

Ozone was prepared in ultra pure oxygen with a silent discharge generator. A mixture of 1000 ppm NO_2 in synthetic air was used as received from Messer Griesheim. 100 % HNO_3 and N_2O_5 were prepared by standard laboratory procedures starting from 65% HNO_3 (Merck, Suprapur), and from NO and ozonized oxygen, respectively. Gaseous $HOONO_2$ (pernitric acid, PNA) was prepared by reacting NO_2BF_4 (97 %, Fluka) with concentrated H_2O_2 (>90 %), and flushed into the chamber immediately to minimize thermal decomposition. The concentrations of NO_2, HNO_3, N_2O_5, PNA and O_3 in the aerosol chamber were measured by long path FTIR spectrometry (Bruker IFS 66v, 112 m folded optical path). NO_3 radical concentrations were measured by FT-Vis spectrometry (Bruker IFS 66/S, 254 m folded optical path). These determinations were complemented by discontinuous *ex situ* measurements with commercial ozone and NO / NO_x monitors (Environment O_3-41M; Horiba APNA-300E; Monitor Labs ML9841). Soot aerosol mass was determined on quartz filters with a commercial carbon analyzer (Ströhlein Coulomat 702). Number densities and size distributions were measured with a condensation nuclei counter (TSI 3022A) and a scanning mobility particle sizer (TSI 3071).

The experiments were analyzed by fitting aerosol size distributions and concentration-time-profiles of the trace gases

with the aerosol physico-chemical simulation code COSIMA (Naumann and Bunz, 1992, 1994). This code describes the dynamics of fractal particles using fractal scaling laws as well as chemical reactions on surfaces and in the gas phase. The modeled processes include particle diffusion, coagulation, sedimentation, gas-to-surface transport including a transition regime correction, surface adsorption and reactions, reactions in the gas phase, and dilution effects due to sampling. The accessible surface area of the fractal particles was calculated as described in Kamm et al. (1999), assuming a primary particle diameter of (5±1) nm (Helsper et al., 1993) and a fractal dimension of 2.0±0.1, which yielded best agreement between model-predicted and measured evolution of the aerosol size distribution and mass.

Results and Discussion

Two sets of experiments were performed to determine the reaction probability of NO_2 on ~200 μg m^{-3} airborne soot at 295 K in dry synthetic air. Both sets consisted of three 5-days-runs in the absence, presence, and absence of soot aerosol. The initial NO_2 concentrations were ~100 ppb. Within the measured uncertainty ranges of the NO / NO_x monitors (±4 ppb and ±2 ppb, respectively) no significant loss of NO_2 or formation of NO could be detected in the presence of soot aerosol during 5 days. This yields an upper limit of $\gamma(NO_2) \leq 4\times10^{-8}$ for the time-averaged reaction probability of NO_2 on soot aerosol. Our $\gamma(NO_2)$ is more than 6 orders of magnitude lower than the initial reaction probability reported by Rogaski et al. (1997), but agrees well with recent results of Longfellow et al. (2000).

The reaction probability of nitric acid on soot aerosol in dry synthetic air was studied likewise in a set of three experiments, each of 48 h duration, using initial concentrations of 500 ppb HNO_3, and 200 μg m^{-3} soot aerosol in the middle run. No significant HNO_3 depletion other than wall loss was observed, and no significant NO_2 formation was detected in the presence of soot aerosol. The combined uncertainties of the analytical procedures yield an upper limit of $\gamma \leq 3\times10^{-7}$ for the time-averaged probability of NO_2 formation. This is ~4 orders of magnitude less than the reactive uptake coefficient reported by Rogaski et al. (1997), but confirms results of Longfellow et al. (2000) and Disselkamp et al. (2000a).

Interactions of N_2O_5 and NO_3 radicals with spark generated soot aerosol were investigated in four different ways: (1) three sets of triplicate experiments were carried out in dry synthetic air, generating NO_3/N_2O_5 *in situ* by mixing similar amounts of NO_2 and ozone in the absence/presence/absence of soot aerosol. This resulted in relatively high NO_3 concentrations; (2) to reduce the relative importance of NO_3 in comparison with N_2O_5, one set of experiments was repeated using a large excess of NO_2 over ozone; (3) in three sets of triplicate experiments, N_2O_5 which had been prepared in the laboratory was added to the dry chamber in the absence / presence / absence of soot aerosol, thereby excluding reactions of ozone with NO_x from an otherwise identical set of chemical reactions; (4) the first experiment (only one triplet) was repeated as described under (1), but at 50% relative humidity to emphasize the loss of N_2O_5 by hydrolysis.

Figure 1A,B depicts the temporal evolution of the trace gas concentrations in the presence and absence of ~200 μg m^{-3} soot aerosol, cases (1) and (2) above. In the presence of soot particles the decay of N_2O_5 and the formation of HNO_3 are significantly faster than in the reference experiments without soot. The model calculations (solid lines), which were used to constrain the heterogeneous reaction probabilities of NO_3 and N_2O_5 on soot particles (see below), are in good agreement with the measurements (symbols). The NO_3 measurements in Figure 1A and similar experiments are in excellent agreement with the simultaneously measured NO_2 and N_2O_5 concentrations only when the most recently measured equilibrium constant for the reaction $NO_2 + NO_3 \leftrightarrow N_2O_5$ is adopted (Wängberg et al., 1997). In Figure 1B the NO_3 concentration was deliberately reduced below the detection limit of the FT-Vis system by adding NO_2 in large (900 ppb) excess of the initial ozone mixing ratio, and only the calculated NO_3 profiles can be shown.

The formation of HNO_3 in the absence of soot aerosol must be due to the reaction of N_2O_5 with water adsorbed on the chamber walls. Since the enhancement of the HNO_3 formation rate is significant in the presence of soot aerosol, we must conclude that an important fraction of N_2O_5 undergoes hydrolysis on the surface of soot particles even at very low humidities (H_2O < 10 ppm in the synthetic air), forming HNO_3, which is released back into the gas phase.

The complete experimental data set of the $N_2O_5/NO_3/NO_2$ system could be fitted with the COSIMA model by including

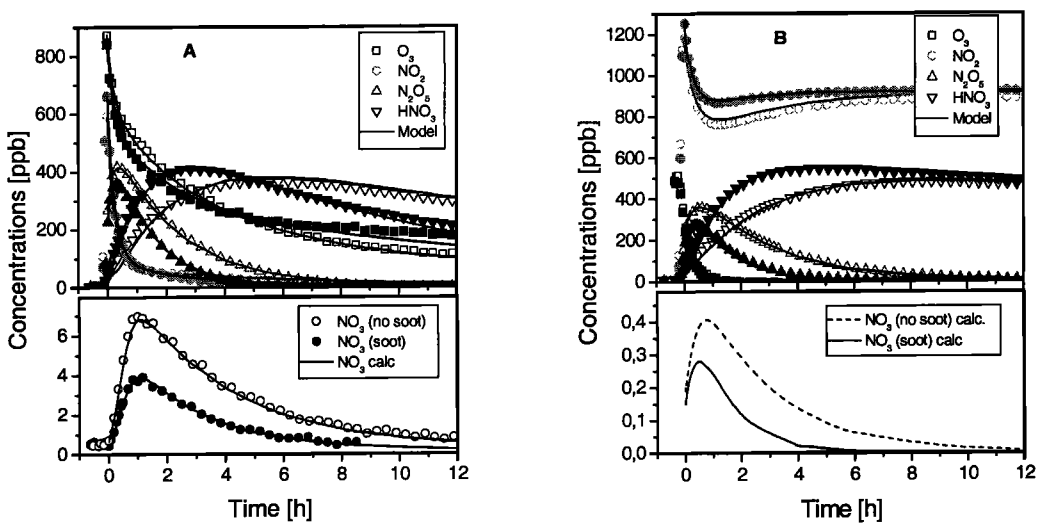

Figure 1. Concentration-time profiles in the presence (filled symbols) and absence (open symbols) of soot aerosol

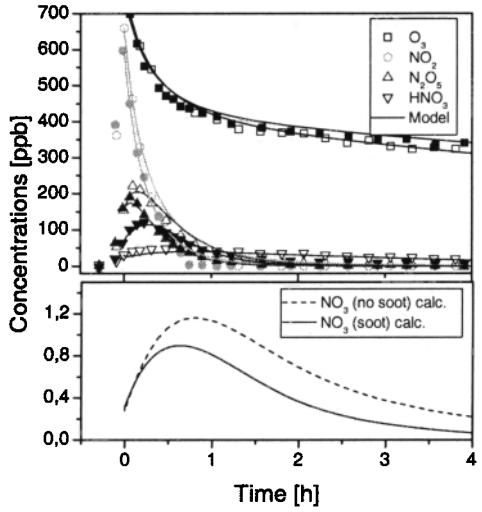

Figure 2. Same as Figure 1A, but at 50% r.h. and 295K

two heterogeneous reactions with the following reaction probabilities, which were assumed to be time independent:

N_2O_5 + soot → 2 HNO_3 $\gamma = (4\pm2)\times10^{-5}$

N_2O_5 + soot → NO + NO_2 + prod. $\gamma = (4\pm2)\times10^{-6}$

The second reaction probability depends on the assumed decomposition mechanism which is, however, not well known (Longfellow et al., 2000). Our data yielded only an upper bound of $\gamma \leq 3\times10^{-4}$ for the reaction probability of NO_3 on soot.

Figure 2 shows concentration-time profiles of reactants and products at 50% relative humidity in the absence / presence of soot aerosol. Although the wall loss of N_2O_5 is much faster compared with the dry system, cf. Figure 1, it was still possible to extract a reaction probability for the hydrolysis rate of N_2O_5 on soot particles:

N_2O_5 + soot (50% r.h.) → 2 HNO_3 $\gamma = (2\pm1)\times10^{-4}$

This is only five times faster than the hydrolysis rate on soot aerosol in "bone dry" air, and two orders of magnitude less than typical reaction probabilities on soluble inorganic aerosol particles at comparable water activities (Mentel et al., 1998), confirming the hydrophobic nature of "clean" soot particles. The fit by the COSIMA model at 50% r.h. is even less sensitive to $\gamma(NO_3)$ on soot, as expected, yielding an upper bound of $\gamma \leq 10^{-3}$.

By adding PNA to the chamber air in the absence / presence of soot aerosol, an upper limit could also be derived for the reaction probability of HO_2 radicals on soot, which exist in equilibrium with PNA and NO_2. Figure 3 shows concentration-time profiles for one set of experiments. Although the overall fit of the COSIMA model was less satisfactory than in previous experiments, the following reaction probabilities have been determined as conservative upper limits:

HO_2 + soot → products $\gamma \leq 10^{-2}$

$HOONO_2$ + soot → products $\gamma \leq 10^{-5}$.

The dashed lines in Figure 3 indicate that significantly larger reaction probabilities for HO_2 are incompatible with our experimental data.

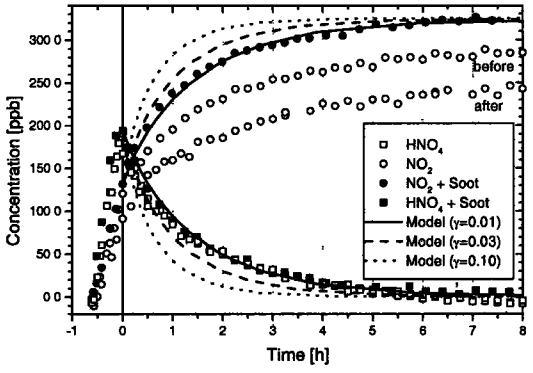

Figure 3. Concentration-time profiles for PNA and NO_2 in the presence (filled symbols) and absence of soot (open symbols, before and after soot experiment)

Atmospheric implications

The impact of soot aerosol surface reactions on the formation of photochemical ozone was investigated by means of box model calculations using the RADM2 chemical code for the gas phase (Stockwell et al., 1990). The initial conditions, diurnal cycles of the photolysis rates and the emissions were identical to the PLUME1 case of a recent model intercomparison exercise (Kuhn et al., 1998). The NO emission rates were varied by factors between 0.01 and 10 to explore the effect of different pollution levels. The surface area concentration of the soot aerosol was assumed to be $C_s = 3\times10^{-3}$ m^{-1} which represents an upper limit. This leads to the following expression for the first order loss rates of reactive species X_i on soot aerosol: $d\ ln\ [X_i]/dt = -\gamma_i\ C_s \langle c_i \rangle / 4$, where $\langle c_i \rangle$ denotes the mean molecular velocity of species X_i. The surface area concentration C_s was assumed to be constant throughout the simulations, which were initially performed for the reference case (*no* reactions on soot), then for each heterogeneous reaction on soot taken into account separately. Finally all reaction probabilities determined in this work were included simultaneously (dry cases only), assuming upper limits of γ in all cases, to be on the safe side, as well as the time dependence of $\gamma(O_3)$ (Kamm et al., 1999). Figure 4 shows ozone maxima for the latter simulations and the reference case, which occurred on the second day of the simulations. The ozone maxima are plotted as function of the NO_y con-

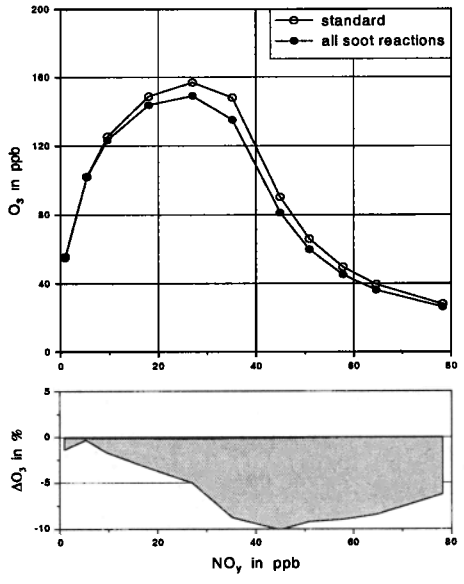

Figure 4. Above: 2nd day ozone maxima, open / filled circles : without / with soot aerosol. Below: % differences in 2nd day ozone maxima

centrations, which had accumulated at the time the ozone maxima had been reached. The wide NO_y range reflects the wide range of NO emission rates, which have been assumed in the calculations.

In the presence as well as in the absence of soot aerosol the ozone maxima on the second day first increase with increasing NO source strength, then decrease again after having passed through a maximum. The chemical conditions below and above the maximum have been termed the low and high NO_x regimes (Vogel et al., 1999). Figure 4 shows that soot has a minor impact on ozone formation in the low NO_x regime, whereas in the high NO_x regime soot may cause ozone reductions of up to 10%. The main contributor is HO_2 (up to 7% reduction in the single compound calculation). This represents an upper bound because the true reaction probability of HO_2 may be lower than the upper limit of 10^{-2} determined in this work.

Considering the extreme assumptions made here (high and constant soot surface area concentration C_s, i.e. no transport, no dilution, no deposition; upper limits of reaction probabilities γ), the impact of soot aerosol on atmospheric chemistry is likely to be small and perhaps negligible.

Acknowledgment: This work, which has been funded by BMBF under grant 07AF209/5, would not have been possible without the continuing support by all staff members of IMK3

References

Aumont B., S. Madronich, M. Ammann, M. Kalberer, U. Baltensperger, D. Hauglustaine, and F. Brocheton, On the NO_2 + soot reaction in the atmosphere, *J. Geophys. Res.*, **104**, 1729-1736, 1999

Bekki, S., On the possible role of aircraft generated soot in the middle latitude ozone depletion. *J. Geophys. Res.*, **102**, 10751-10758, 1997

Brouwer L., M.J. Rossi, and D.M. Golden, Reaction of N_2O_5 with H_2O on Carbonaceous Surfaces,. *J. Phys. Chem.*, **90**, 4599-4603, 1986

Disselkamp, R.S., M.A. Carpenter, and J.P. Cowin, A Chamber Investigation of Nitric Acid – Soot Aerosol Chemistry at 298 K, *J. Atmos. Chem.*, **37**, 113-123, 2000a

Disselkamp, R.S., M.A. Carpenter, J.P. Cowlin, C.M. Berkowitz, E.G. Chapman, R.A. Zaverin and N.S. Laulainen, Ozone loss in soot aerosol. *J. Geophys. Res.*, **105**, 9767-9771, 2000b

Fendel, W., D. Matter, H. Burtscher, A. Schmidt-Ott, Interaction between carbon or iron aerosol particles and ozone. *Atmos. Environ.* **29**, 967-973, 1995

Hansen, J., M. Sato, R. Ruedy, A. Lacis and V. Oinas, Global warming in the twenty-first century: An alternative scenario. *Proc. Natl. Acad. Sci.* **97**, 9875-9880, 2000

Hauglustaine, D.A., B.A. Ridley, S. Solomon, P.G. Hess, and S. Madronich, HNO_3/NO_x ratio in the remote troposphere during MLOPEX 2: Evidence for nitric acid reduction on carbonaceous aerosols, *Geophys. Res. Lett.*, **23**, 2609-2612, 1996

Helsper, C., W. Mölter, F. Löffler, C. Wadenpohl, S. Kaufmann and G. Wenninger, Investigation of a new aerosol generator for the production of carbon aggregate particles. *Atmos. Environ.* **27A**, 1271-1275, 1993

Israel G.W., C. Schlums, R. Treffeisen und M. Pesch, *Rußimmission in Berlin.* Final Report B 281 KF, VDI Verlag GmbH, Düsseldorf 1996

Jacob D. J., Heterogeneous chemistry and tropospheric ozone, *Atmos. Environ.*, **34**, 2131-2159, 2000

Jacobson, M.Z., A physically-based treatment of elemental carbon optics: implications for global direct forcing of aerosols. *Geophys. Res. Lett.*, **27**, 217-220, 2000

Kalberer M., K. Tabor, M. Ammann, Y. Parrat, E. Weingartner, D. Piguet, E. Rössler, D.T. Jost, A. Türler, H.W. Gäggeler, and U. Baltensperger, Heterogeneous Chemical Processing of $^{13}NO_2$ by Monodisperse Carbon Aerosols at Very Low Concentrations, *J. Phys. Chem.* **100**, 15487-15493, 1996

Kamm, S., O. Möhler, K.-H. Naumann, H. Saathoff, and U. Schurath, The Heterogeneous Reaction of Ozone with Soot Aerosol, *Atmos. Environ.* **33**, 4651-4661, 1999

Kirchner, U., V. Scheer and R. Vogt, FTIR spectroscopic investigation of the mechanism and kinetics of the heterogeneous reactions of NO_2 and HNO_3 with soot. *J. Phys. Chem.*, **A104**, 8908-8915, 2000

Kuhn M., D. Poppe, Y. Andersson-Sköld, A. Baart, P.J.H. Builtjes, M. Das, F. Fiedler, O. Hov, F. Kirchner, P.A. Makar, J.B. Milford, M.G.M. Roemer, R. Ruhnke, D. Simpson, W.R. Stockwell, A. Strand, B. Vogel, H. Vogel, Intercomparison of the Gas Phase Chemistry in Several Chemistry and Transport Models, *Atmos. Environ.*, **32**, 693-798, 1998

Lary, D.J., Toumi, R., Lee, A.M., Newchurch, M., Pirre, M., and Renard, J.B., Carbon aerosols and atmospheric photochemistry. *J. Geophys. Res.*, **102** (D3) 3671-3682, 1997

Longfellow, C.A., A.R. Ravishankara and D.R. Hanson, Reactive and nonreactive uptake on hydrocarbon soot: HNO_3, O_3, and N_2O_5. *J. Geophys. Res.* **105**, 24345-24350, 2000

Mentel, T.F., M. Sohn, and A. Wahner, Nitrate effect in the heterogeneous hydrolysis of dinitrogen pentoxide on aqueous aerosols, *Phys. Chem. Chem. Phys.*, **1**, 5451-5457, 1999

Naumann, K.-H. and H. Bunz, Computer simulations on the dynamics of fractal aerosols. *J. Aerosol Sci.*, **23** 361-364, 1992

Naumann, K.-H. und H. Bunz, Eine theoretische Verbindung zwischen dem Formfaktorkonzept und der fraktalen Beschreibung irregulär strukturierter Partikel. *KfK Report 5275*, 1994

Pakkanen, T.A., V.M. Kerminen, Ch.H. Ojanen, R.E. Hillamo, P. Aarnio and T. Koskentalo, *Atmos. Environ.*, **34**, 1497-1506, 2000

Petzold, A., J. Ström, F.P. Schröder and B. Kärcher, *Atmos. Environ.*, **33**, 2689-2698, 1999

Rogaski, C.A., D.M. Golden, and L.R. Williams, Reactive uptake and hydration experiments on amorphous carbon treated with NO_2, SO_2, O_3, HNO_3, and H_2SO_4. *Geophys. Res. Lett.*, **24**, 381-384, 1997

Stephens, S., M.J. Rossi and D.M. Golden, The heterogeneous reaction of ozone on carbonaceous surfaces. *Int. J. Chem. Kinet.*, **18**, 1133-1149, 1986

Stockwell, W.R., P. Middleton, J.S. Chang, X. Tang, The second generation regional acid deposition model chemical mechanism for air quality modeling, *J. Geophys. Res.*, **95**, 16343-16368, 1990

Strawa, A.W., K. Drdla, G.V. Ferry, S. Verma, R.F. Pueschel, M. Yasuda, R.J. Salawich, R.S. Gao, S.D. Howard, P.T. Bui, M. Loewenstein, J.W. Elkins, K.K. Perkins and R. Cohen, *J. Geophys. Res.*, **104**, 26753-26766, 1999

Underwood, G.M., P. Li, C.R. Usher and V.H. Grassian, Determining accurate kinetic parameters of potentially important heterogeneous atmospheric reactions on solid particle surfaces with a Knudsen cell reactor, *J. Phys. Chem.*, **A104**, 819-829, 2000

Vogel, B., F. Fiedler, H. Vogel, Influence of topography and biogenic volatile organic compounds emission in the state of Baden-Württemberg on ozone concentrations during episodes of high air temperatures. *J. Geophys. Res.*, **100**, 22907-22928, 1995

Wängberg, I., T. Etzkorn, I. Barnes, U. Platt and K.H. Becker, Absolute determination of the temperature behaviour of the NO_2 + NO_3 +(M) $\leftrightarrow$ N_2O_5 +(M) equilibrium. *J. Phys. Chem.* **A101**, 9694-9698, 1997

H. Saathoff, K.-H. Naumann, N. Riemer, S. Kamm, O. Möhler, U. Schurath, H. Vogel and B. Vogel, FZK, Institut für Meteorologie und Klimaforschung, POB 3640, D-76021 Karlsruhe, Germany. E-mail: harald.saathoff@imk.fzk.de, naumann@imk.fzk.de, schurath@ imk.fzk.de, vogel@imk.fzk.de

(Received November 13, 2000; revised February 16, 2001; accepted February 19, 2001)